Supporting Information

Sánchez-Iranzo et al. 10.1073/pnas.1716713115

SI Materials and Methods

Transgenic Lines. The construct to generate Tg(*postnb*:citrine)^{cn6} was obtained by recombining the iTol2Amp cassette (1) followed by the citrine-Kan cassette (Table S1, primers 3 and 4) into the BAC CH211-38D6. The construct for Tg(*periostin:CreER^{T2}*)^{cn7} was generated by recombining the *iTol2Amp-Cryst:GFP* cassette (Table S1, primers 9 and 10 and Dataset S5) followed by *CreERT2-frt-Kan-frt* (2) (Table S1, primers 5 and 6) into the BAC CH73-370H18. The plasmid to generate Tg(*col1a2:loxP-tagBFP-loxP-mCherry-NTR*)^{cn8} was obtained by recombining the *iTol2-CrystCFP* (3) (Table S1, primers 7 and 8) and *loxP-tagBFP-loxP-mCherry-NTR* (2) (Table S1, primers 1 and 2) cassettes into the BAC CH211-122K13. Once the transgenic line was established, *Cre recombinase* mRNA was injected at 50 ng·μL^{-1} to recombine the *loxP* sites to generate Tg(*col1a2:loxP-mCherry-NTR*)^{cn11}.

The plasmid to generate the Tg(*fli1a:CreER^{T2}*)^{cn9} line was obtained using Gateway (4) to recombine the plasmids p5E-fli1ep (5), pME-CreER^{T2} (6), and p5E-pA (4) into the pDestTol2pA2 (5) backbone (Dataset S6).

Plasmid templates for recombineering and the plasmid to generate the Tg(*wt1a:CreER^{T2}*)^{cn10} line were cloned using Gibson Assembly (NEB) using the promoter reported previously (7) (Dataset S7). Recombineering was performed by combining the pRedET (Gene Bridges) system and EL250 bacteria (8). DNA was injected at 25 ng·μL^{-1} into one-cell-stage zebrafish embryos along with 1 nL of 50 ng·μL^{-1} synthetic *Tol2* mRNA in Danieau buffer.

Other lines used were Tg(*kdrl:mcherry*) (kindly provided by E. Ober, Copenhagen), Tg(-3.5*ubb:loxP-loxP-eGFP*)^{cz1702Tg} (6), Tg(*ubb:Switch*)^{cz1701} (6), Tg(*ubb:mCherry*)^{cz1705Tg} (6), Tg(*fli1a:GFP*)^{y1} (9), Tg1(*-6.8wt1a:EGFP*)^{li7Tg} (7), and Tg(*tcf21:CreER^{T2}*)^{pd42Tg} (10).

In adults, 10 μM 4-OHT was administered at the indicated times dissolved in 100 mL of fish water per fish. Treatments were performed overnight for 12 h. Before administration, the 10 mM stock (dissolved in ethanol) was heated for 10 min at 65 °C (11). In embryos, it was administered at 5 μM. Cryoinjury was performed as previously described (12). Genetic ablation was performed using the nitroreductase system previously described (13). Metronidazole (Sigma) was added at 10 mM to fish water at the indicated times.

Whole-Kidney Marrow Transplantation. Transplantations were performed as described (14).

Histology and Sectioning. Samples for Figs. 1 *C–F* and 5 and Figs. S4, S6, S8, and S9 *G–M* were fixed in 4% paraformaldehyde (PFA) in PBS overnight at 4 °C, washed in PBS + 0.1% Tween 20 (Sigma), dehydrated through an ethanol series, and embedded in paraffin. They were sectioned at 7 μm with a microtome (Leica), mounted on Superfrost slides (Fisher Scientific), and dried overnight at 37 °C. Sections were deparaffinized in xylol, rehydrated, and washed in distilled water. Connective tissue was stained using acid fuchsin orange G (AFOG). For analysis of the amount of IA/IA + myocardium (Fig. S8), the total ventricular tissue area and IA on all sections on a slide of each heart (collected on five slides) were measured.

Other sections were processed by fixing in 4% PFA and washing in PBS + 0.1% Tween 20. They were then incubated in 15% saccharose overnight at 4 °C, embedded in 30% gelatin, 15% saccharose, and snap-frozen at −80 °C in isopentane. They were cut at 8 μm on a cryostat (Leica).

For immunofluorescence, whole-mount hearts were fixed in 4% PFA overnight, washed in PBS + 0.1% Tween, and permeabilized with PBS + 0.5% Triton X-100 (Sigma) for 20 min. Several washing steps were followed by at least 2 h of blocking with 5% goat serum, 5% BSA, 20 mM $MgCl_2$ in PBS, and then slides were incubated with the antibodies overnight.

Paraffin sections were deparaffinized, rehydrated, and washed in distilled water. Epitopes were retrieved by heating in 10 mM citrate buffer (pH 6.0) for 15 min in a microwave oven at full power. Gelatin sections were incubated for 30 min in PBS + 0.1% Tween 20 at 37 °C to dissolve the gelatin. Nonspecific binding sites were saturated by incubation for at least 1 h in blocking solution (as above). Endogenous biotin was blocked with the Avidin/Biotin Blocking Kit (Vector).

In situ hybridization was performed using *col1a2* and *postnb* riboprobes (15).

Primary antibodies used were anti-myosin heavy chain (DSHB, MF20, 1:20; DSHB, F59, 1:20), anti-GFP (Aves, GFP-1010, 1:500; Clontech, 632592, 1:100), anti-col1a1 (DSHB, SP1.D8, 1:20), anti-RFP (Abcam, ab34771, 1:200), anti–Mef-2 (Santa Cruz Biotechnology, C21, sc-313, 1:200), and anti-BrdU (BD Biosciences, B44, 1:100), and biotin- or Alexa (488, 568, 633)-conjugated secondary antibodies and streptavidin-Cy3 (Jackson ImmunoResearch) were used at 1:300. Nuclei were stained with DAPI and slides were mounted in FluorSave (Calbiochem).

Quantitative Real-Time PCR. RNA from cardiac ventricles was extracted using 0.5 mL TRIzol reagent (Ambion, Life Technologies). One ventricle was used per biological replicate. RNA was transcribed to cDNA using the High-Capacity cDNA Reverse Transcription Kit (Applied Biosystems, Life Technologies). qRT-PCR was performed using Power SYBR Green PCR Master Mix (Applied Biosystems). *col1a2* and *postnb* expression was normalized to the geometric mean of the expression level of two constitutive genes, *EF1-alpha* and *rps11*. Primer information is available in Table S2.

Heart Dissociation, Sorting, and RNA-Seq Library Production. For Tg (*kdrl:mCherry;postnb:citrine*) fish, the apex of the heart was dissected and dissociated for 45 min in trypsin. Whole ventricles [for Tg(*wt1a:GFP*)] or apices—for Tg(*postnb:CreERT2;ubi:Switch*)—were dissected and dissociated according to previous protocols (16) with minor modifications: The enzyme concentration was doubled and time of digestion was increased to 2 h. Then, one volume of PBS + 10% FBS was added to the sample, which was centrifuged for 8 min at 250 × *g* and resuspended in PBS + 1% FBS.

Cell Sorting and RNA-Seq Library Production. Cells were sorted on a Synergy SY3200 cell sorter (Sony Biotechnology) and RNA was extracted using the Arcturus PicoPure Kit (Thermo Fisher Scientific). Pools of three to five apices per ventricle were used.

For *kdrl*:mCherry^{+} cells, three pools of three to five hearts were used for the uninjured condition, and five pools of three to five hearts were used for the 7 dpi condition. Three pools of three to five ventricular apices were used for *postnb*:citrine cells per condition, and six pools of three to five ventricular apices were used for the remainder of the cells. For *postnb*-derived cells, four pools of three to five hearts were used for 7 dpi, and three pools were used for 60 dpi.

Total RNA (0.25 to 1 ng) was used to generate barcoded RNA-seq libraries using the Ovation Single Cell RNA-Seq System

(NuGEN) with two rounds of library amplification. The size of the libraries was calculated using the Agilent 2100 Bioanalyzer. Library concentration was determined using the Qubit fluorometer (Thermo Fisher Scientific). Libraries were sequenced on the HiSeq 2500 System (Illumina) to generate 60-base single reads. FastQ files for each sample were obtained using CASAVA v1.8 software (Illumina). Four biological replicates consisting of five pooled hearts were used per sample.

RNA-Seq Analysis. Sequencing adaptor contaminations were removed from reads using cutadapt 1.9.1 software (17), and the resulting reads were mapped and quantified on the transcriptome (Ensembl gene-build 10, release 82) using RSEM v1.2.25 (18). Only genes with at least one count per million in at least two or three samples were considered for statistical analysis. Data were then normalized and differential expression was tested using the Bioconductor package edgeR (19). We considered as differentially expressed those genes with a Benjamini–Hochberg adjusted P value ≤ 0.05 and LFC ≥ 1. For the Tg(*wt1a:GFP*) samples, paired analysis was used. Heatmaps were made using gplot library and heatmap.2 function.

1. Suster ML, Abe G, Schouw A, Kawakami K (2011) Transposon-mediated BAC transgenesis in zebrafish. *Nat Protoc* 6:1998–2021.
2. Sánchez-Iranzo H, et al. (2018) Tbx5a lineage tracing shows cardiomyocyte plasticity during zebrafish heart regeneration. *Nat Commun* 9:428.
3. Donà E, et al. (2013) Directional tissue migration through a self-generated chemokine gradient. *Nature* 503:285–289.
4. Kwan KM, et al. (2007) The Tol2kit: A multisite Gateway-based construction kit for Tol2 transposon transgenesis constructs. *Dev Dyn* 236:3088–3099.
5. Villefranc JA, Amigo J, Lawson ND (2007) Gateway compatible vectors for analysis of gene function in the zebrafish. *Dev Dyn* 236:3077–3087.
6. Mosimann C, et al. (2011) Ubiquitous transgene expression and Cre-based recombination driven by the ubiquitin promoter in zebrafish. *Development* 138: 169–177.
7. Bollig F, et al. (2009) A highly conserved retinoic acid responsive element controls wt1a expression in the zebrafish pronephros. *Development* 136:2883–2892.
8. Lee EC, et al. (2001) A highly efficient *Escherichia coli*-based chromosome engineering system adapted for recombinogenic targeting and subcloning of BAC DNA. *Genomics* 73:56–65.
9. Lawson ND, Weinstein BM (2002) In vivo imaging of embryonic vascular development using transgenic zebrafish. *Dev Biol* 248:307–318.
10. Kikuchi K, et al. (2011) tcf21^{+} epicardial cells adopt non-myocardial fates during zebrafish heart development and regeneration. *Development* 138:2895–2902.
11. Felker A, et al. (2016) In vivo performance and properties of tamoxifen metabolites for CreERT2 control. *PLoS One* 11:e0152989.
12. González-Rosa JM, Mercader N (2012) Cryoinjury as a myocardial infarction model for the study of cardiac regeneration in the zebrafish. *Nat Protoc* 7:782–788.
13. Curado S, Stainier DY, Anderson RM (2008) Nitroreductase-mediated cell/tissue ablation in zebrafish: A spatially and temporally controlled ablation method with applications in developmental and regeneration studies. *Nat Protoc* 3:948–954.
14. Li P, et al. (2015) Epoxyeicosatrienoic acids enhance embryonic haematopoiesis and adult marrow engraftment. *Nature* 523:468–471.
15. González-Rosa JM, Peralta M, Mercader N (2012) Pan-epicardial lineage tracing reveals that epicardium derived cells give rise to myofibroblasts and perivascular cells during zebrafish heart regeneration. *Dev Biol* 370:173–186.
16. Tessadori F, et al. (2012) Identification and functional characterization of cardiac pacemaker cells in zebrafish. *PLoS One* 7:e47644.
17. Martin M (2011) Cutadapt removes adapter sequences from high-throughput sequencing reads. *EMBnet J* 17:10–12.
18. Li B, Dewey CN (2011) RSEM: Accurate transcript quantification from RNA-seq data with or without a reference genome. *BMC Bioinformatics* 12:323.
19. Robinson MD, McCarthy DJ, Smyth GK (2010) edgeR: A Bioconductor package for differential expression analysis of digital gene expression data. *Bioinformatics* 26: 139–140.

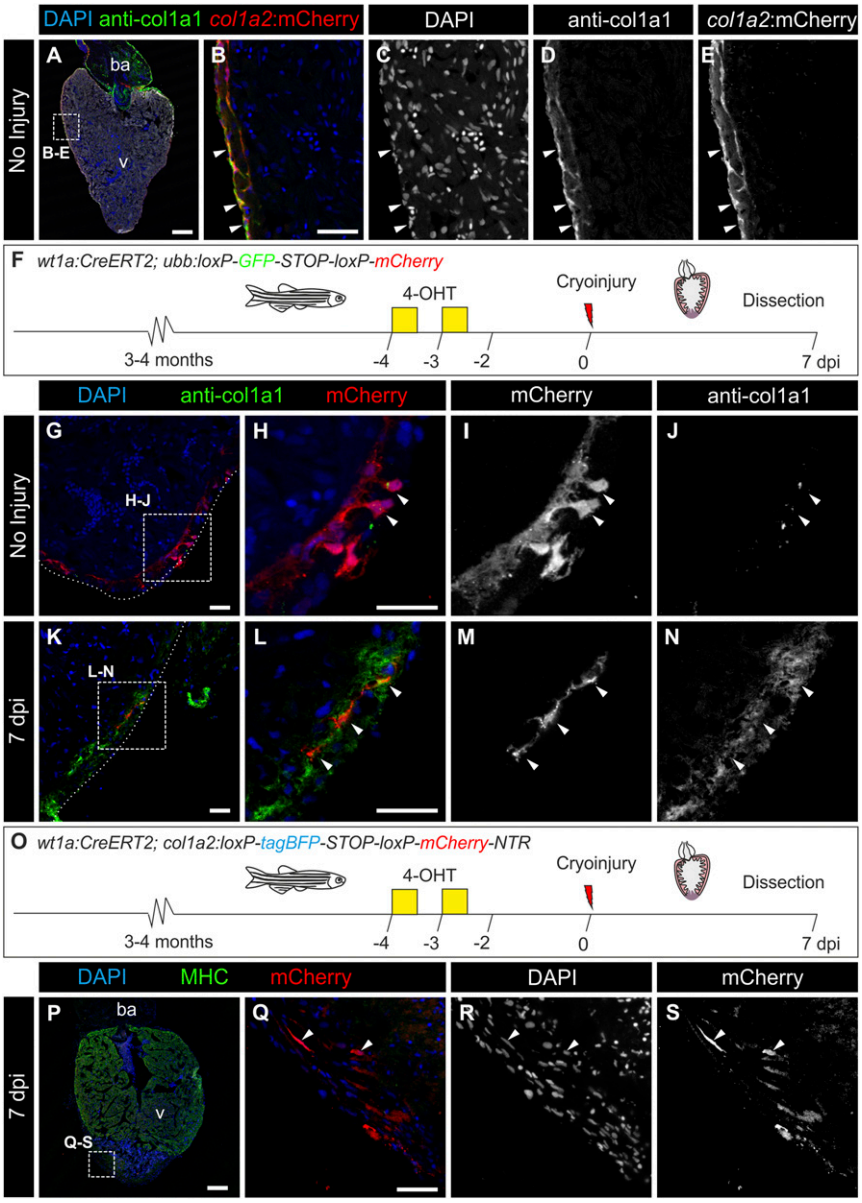

Fig. S1. *col1a2:mCherry-NTR* transgenic line allows the labeling of collagen-producing cells, and *wt1a*-derived cells express *col1a2* after cryoinjury. (*A*) Immunofluorescence of heart sections with anti-col1a1 (green) and mCherry (red). Nuclei are counterstained with DAPI. (*B–E*) Merged and individual channels of the boxed area in *A*. Arrowheads mark mCherry$^+$ cells that are surrounded by col1a1. (*F–N*) Lineage tracing of *wt1a*$^+$ cells. (*F*) 4-Hydroxytamoxifen (4-OHT) was added to adult *wt1a:CreER*^{T2}*;ubb:Switch* uninjured fish 10 and 9 d before dissection. (*G–N*) Immunofluorescence staining with anti-col1a1 (green) and mCherry (red) of heart sections of uninjured hearts (*G–J*) or 7 d postinjury (dpi) hearts (*K–N*). Nuclei are DAPI-counterstained (blue). Arrowheads mark *wt1a*-derived cells. (*O*) Experimental scheme for tracing the fate of *wt1a*-derived cells expressing *col1a2*. The *wt1a:CreER*^{T2} line was crossed with the *col1a2:loxP-tagBFP-STOP-loxP-mCherry-NTR* line, in which mCherry-NTR is not expressed. Upon 4-OHT administration, recombination of loxP sites leads to activation of mCherry expression under the control of a *col1a2* promoter. Hearts from animals at 7 dpi were dissected and sectioned. (*P–S*) Immunofluorescence of heart sections with anti-myosin heavy chain (MHC; green), and mCherry (red). Nuclei are counterstained with DAPI. (*Q–S*) Merged and individual channels of the boxed area in *P*. Arrowheads mark mCherry$^+$ cells, which express *col1a2*. ba, bulbus arteriosus; v, ventricle. [Scale bars, 25 μm (*B*, *G*, *H*, *K*, *L*, and *Q*) and 100 μm (*A* and *P*).]

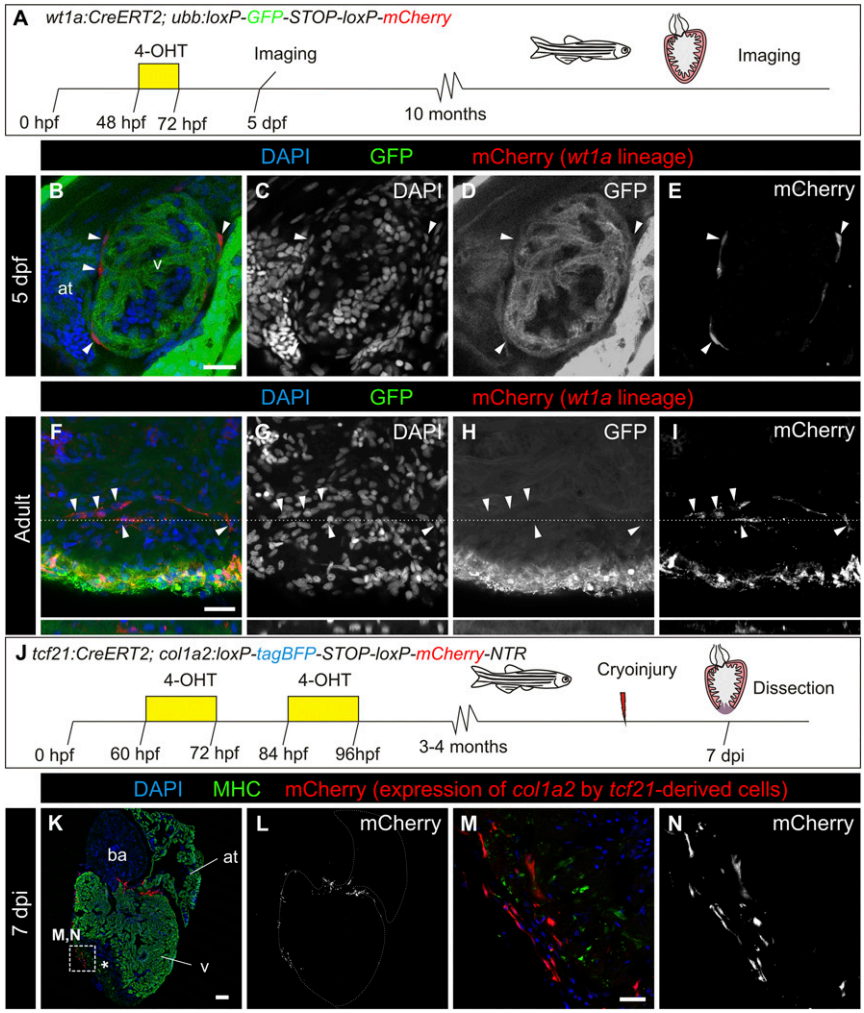

Fig. S2. Resident fibroblasts are derived from the epicardium, and cells derived from the epicardium and resident fibroblasts express *col1a2*:mCherry after injury. (*A*) Experimental scheme for tracing the fate of *wt1a*-derived cells. 4-OHT was administered from 48 to 72 h postfertilization (hpf). (*B–E*) Immunofluorescence of 5 d postfertilization (dpf) embryos with anti-GFP (green) and mCherry (red). Nuclei are counterstained with DAPI. (*C–E*) Single channels of the merged image shown in *B*. (*F–I*) Immunofluorescence of whole-mount adult hearts with anti-GFP (green) and mCherry (red). Nuclei are counterstained with DAPI. Orthogonal views of the plane highlighted with dotted lines are shown below. Shown are single (*G–I*) and merged (*F*) channels. (*J*) Experimental scheme for tracing the fate of *tcf21*-derived cells expressing *col1a2*. The *tcf21:CreER*^{T2} line was crossed with the *col1a2:loxP-tagBFP-STOP-loxP-mCherry-NTR* line. Upon 4-OHT administration, recombination of loxP sites leads to activation of mCherry expression under the control of a *col1a2* promoter. Hearts from animals at 7 dpi were dissected and sectioned. (*K–N*) Immunofluorescence of the heart sections with anti-MHC (green) and mCherry (red). Nuclei are counterstained with DAPI. Asterisk indicates injured area. (*M* and *N*) Merged and individual channels of the boxed area in *K*. Arrowheads mark mCherry^{+} cells, which express *col1a2*. at, atrium. [Scale bars, 25 μm (*B*, *F*, and *M*) and 100 μm (*K*).]

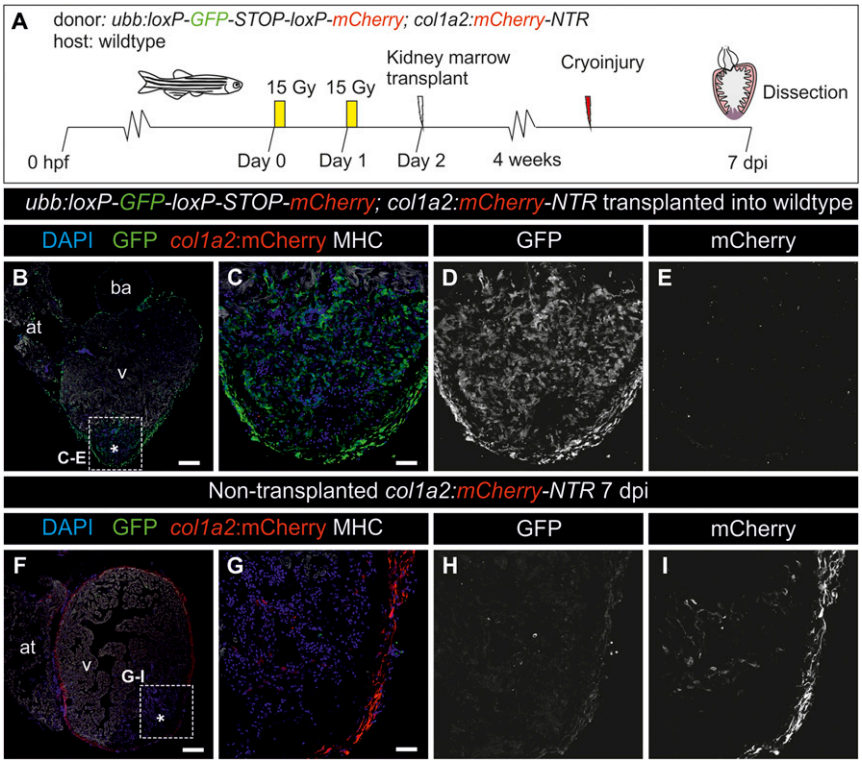

Fig. S3. Kidney marrow-derived cells do not contribute to collagen deposition during fibrotic response to cryoinjury. (*A*) Kidney marrow-derived cells from a transgenic line ubiquitously expressing GFP and mCherry under the control of *col1a2* regulatory regions were transplanted into irradiated wild-type adult zebrafish. After kidney marrow reconstitution, host hearts were cryoinjured. Expression of mCherry and GFP was assessed at 7 dpi by immunofluorescence of sections. MHC marks the myocardium, and nuclei are counterstained with DAPI. (*B*) Whole-heart section of a transplanted heart at 7 dpi. (*C*–*E*) Merged and single channels of the boxed area in *B*. No mCherry signal is visible. (*F*) Control whole-heart section from a *col1a2:mCherry* transgenic fish at 7 dpi. (*G*–*I*) Merged and single channels of the boxed section shown in *F*; mCherry signal is detected in the epicardium and injury areas. Asterisks indicate the injury area. [Scale bars, 25 μm (*C* and *G*) and 100 μm (*B* and *F*).]

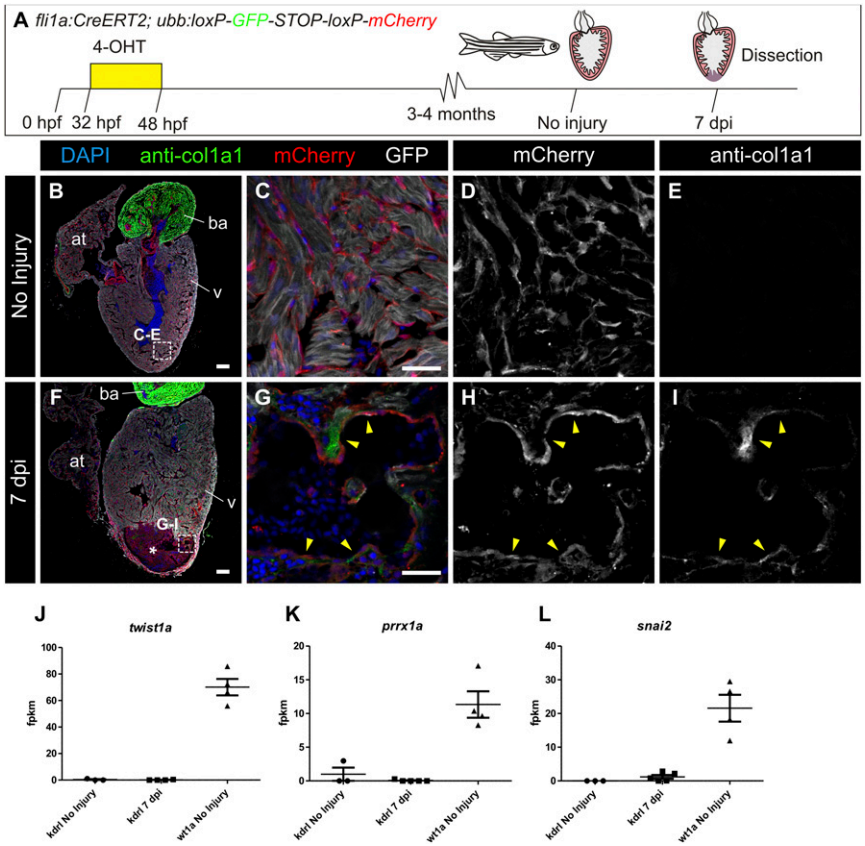

Fig. S4. Endocardial cells at the injury area express collagen 1a1 but not EMT markers. (*A–I*) Lineage tracing of endocardial cells in the uninjured and injured heart. (*A*) Experimental scheme for tracing the contribution of endocardial cells to fibrosis using the *ubb:Switch* reporter line. (*B* and *F*) Immunofluorescence staining of whole-heart sagittal sections (*B*, uninjured; *F*, 7 dpi) with anti-mCherry (red), anti-col1a1 (green), and anti-MHC (gray); nuclei were DAPI-counterstained (blue). *C–E* and *G–I* are merged and single channels of a zoomed-in view of the endocardial border in the apex or close to the injury area (IA; asterisk). *fli1a*-derived cells are mCherry$^+$ (red). Note that at 7 dpi, mCherry$^+$ cells (red) are closely associated with col1a1 (green) deposits (arrowheads). (*J–L*) Epithelial-to-mesenchymal transition (EMT) markers are expressed by *wt1a*:GFP$^+$ cells but not by *kdrl*:mCherry$^+$ cells. Graphs show the fragments per kilobase million (fpkm) values for the same genes and samples. Shown are individual measurements as well as mean and SD. EMT genes were more abundant in *wt1a*$^+$ cells than in *kdrl*$^+$ cells both before and after injury. [Scale bars, 25 μm (*C* and *G*) and 100 μm (*B* and *F*).]

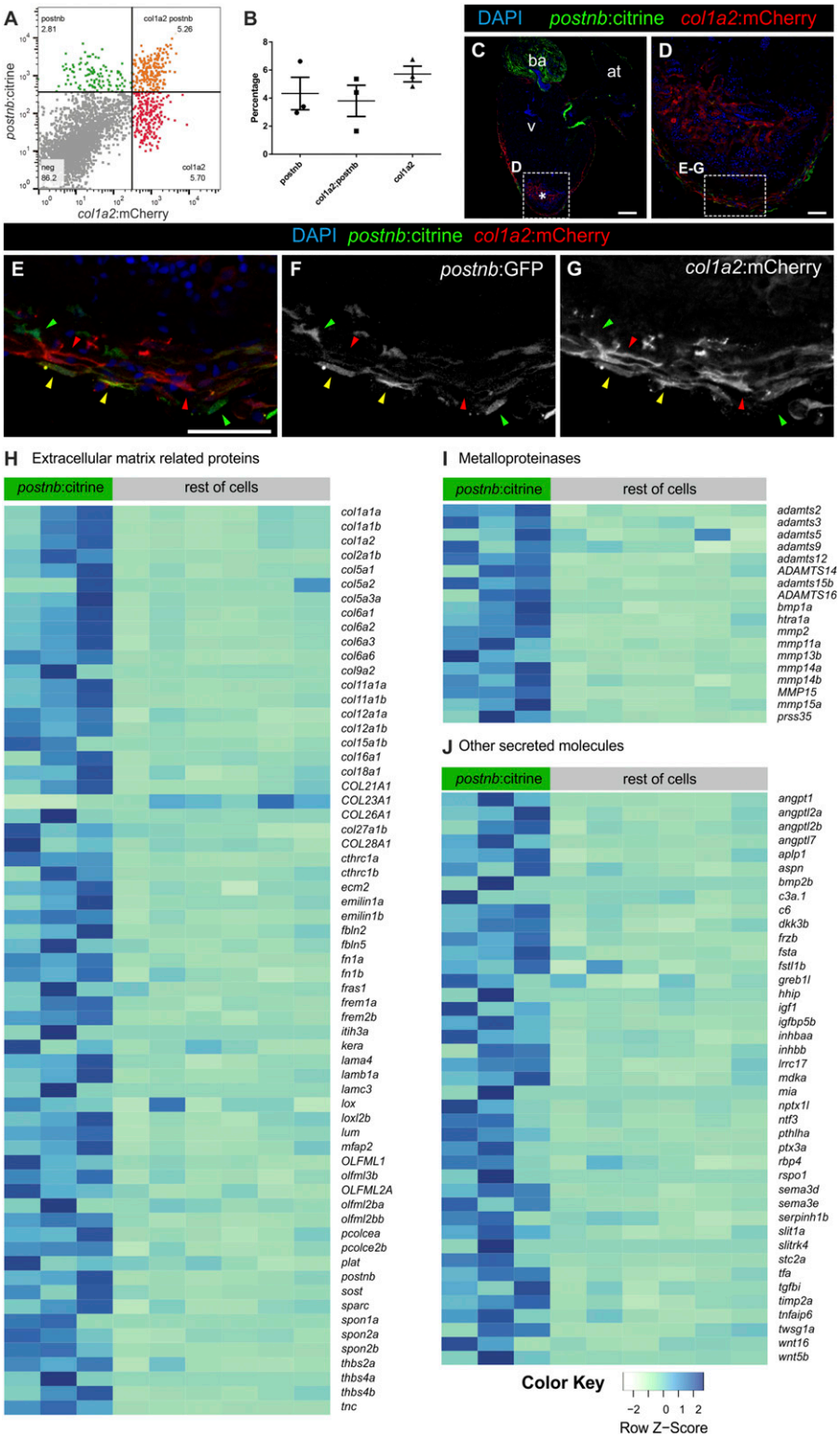

Fig. S5. Colocalization of *postnb*:citrine^{+} and *col1a2*:mCherry^{+} cells. (*A* and *B*) FACS-sorted cells of 7 dpi hearts from *co1a2:mCherry;postnb:citrine* double-transgenic fish. Based on these markers, three populations could be detected: double-positive, *postnb*$^{+}$, and *col1a2*$^{+}$. Shown are individual measurements as well as mean and SD. (*C–G*) Immunofluorescence with anti-GFP (green) and anti-mCherry (red) of a heart section from an adult *postnb:citrine;col1a2:mCherry-NTR* fish. Note the presence of double-positive (yellow arrowheads), *col1a2*$^{+}$ (red arrowheads), and *postnb*$^{+}$ cells (green arrowheads). (*H–J*) Heatmaps representing the expression levels of all of the secreted proteins that were identified to be up-regulated when comparing *postnb*:citrine^{+} cells at 7 dpi with the rest of the cells at the injury (with the exception of the *kdrl*:mCherry population). Fragments per kilobase million values were used. The list of genes encoding secreted molecules was obtained by using Ingenuity software and manually adding the genes encoding for collagens and metalloproteinases not identified by Ingenuity. For better visualization of changes in gene expression between the two groups, values were scaled independently for each gene, that is, each row. [Scale bars, 25 μm (*C*) and 100 μm (*D* and *E*).]

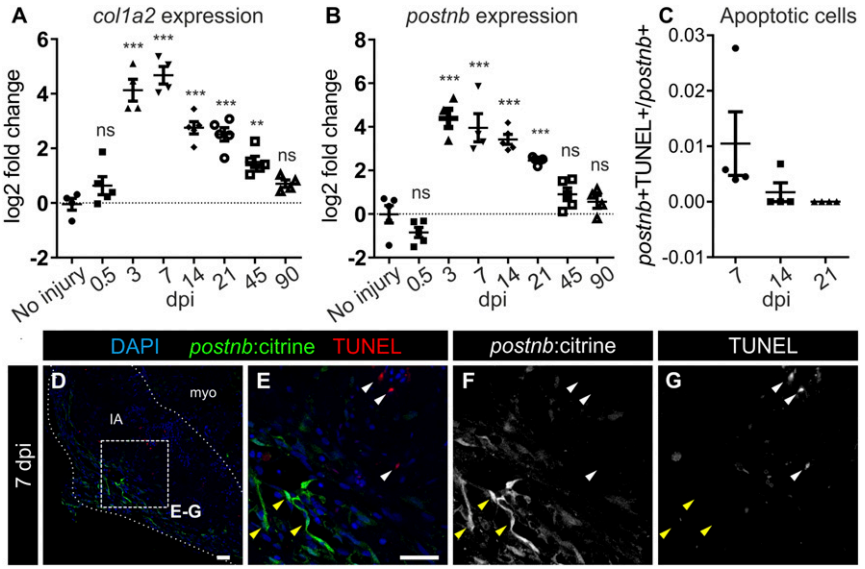

Fig. S6. Apoptotic and senescent fibroblasts during heart regeneration. (*A* and *B*) qPCR of *col1a2* and *postnb* at different days postinjury. Symbols show data for individual samples; bars and whiskers show mean ± SD; ***$P < 0.001$, **$P < 0.01$ by one-way ANOVA followed by Tukey's multiple comparisons test. ns, not significant. (*C*) *postnb*$^+$ apoptotic (TUNEL$^+$) cell quantification. (*D*–*G*) TUNEL staining of *postnb*:citrine heart sections. myo, myocardium. *pstnb*:citrine$^+$ cells, yellow arrowheads; TUNEL$^+$ cells, white arrowheads. (Scale bars, 25 μm.)

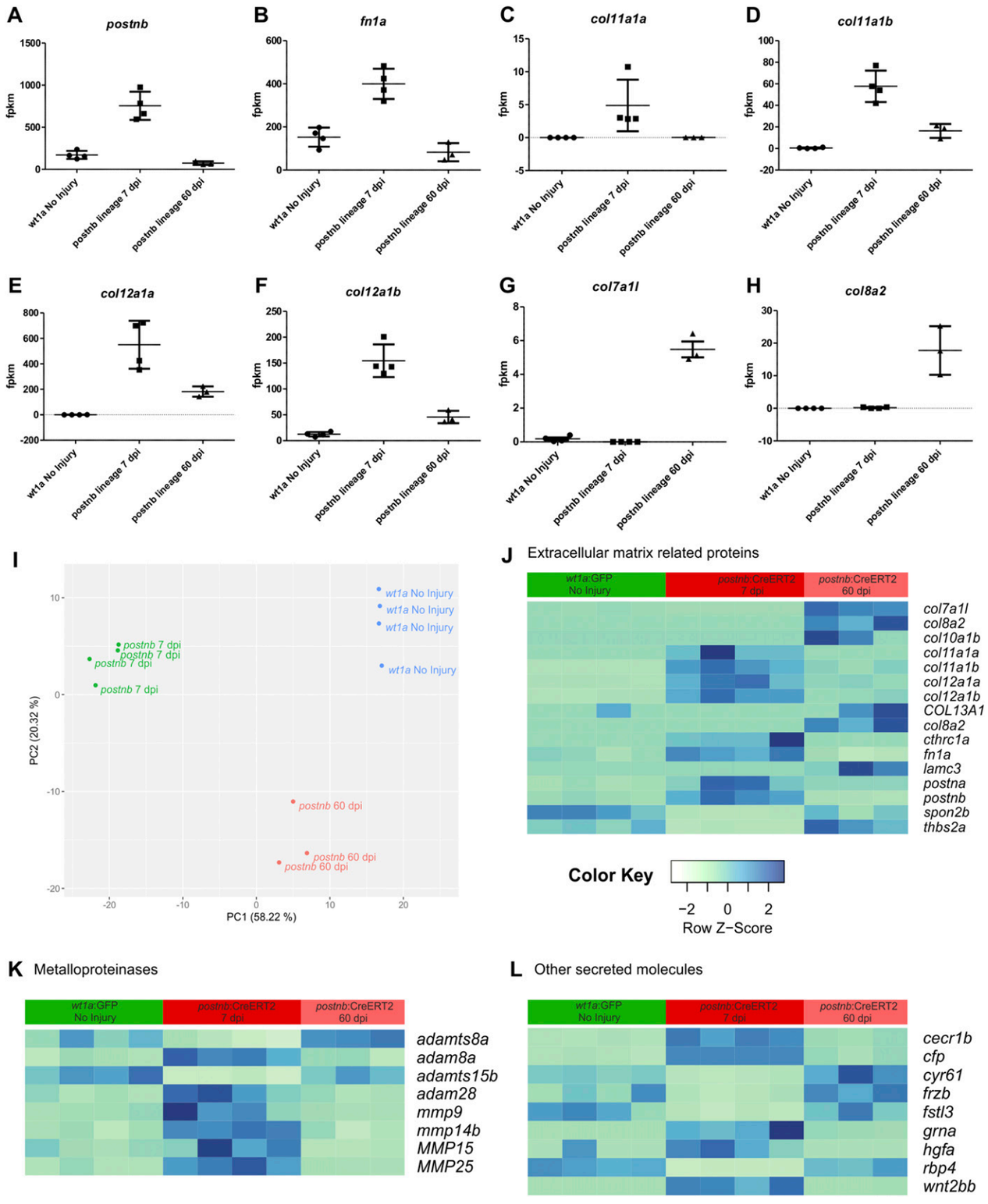

Fig. S7. Comparison of the gene expression profiles of resident intracardiac fibroblasts, activated fibroblasts, and inactivated fibroblasts. (*A*–*H*) Plots of fragments per kilobase million (fpkm) values for the same genes and samples: Extracellular matrix genes were more abundant in *postnb*-derived cells at 7 dpi. Shown are individual measurements as well as mean and SD. In some cases, the expression profile of *wt1a*:GFP- and *postnb*-derived cells at 60 dpi did not coincide, suggesting that fibroblasts do not fully revert to a quiescent state during heart regeneration. The genes up-regulated in *postnb*-derived cells at 60 dpi are expressed at low levels. (*I*) Principal component (PC) analysis of RNA-seq samples from uninjured *wt1a*:GFP^{+} cells and *postnb*-derived cells from hearts at 7 and 60 dpi. (*J*–*L*) Heatmaps representing the expression levels of all of the secreted proteins that were identified to be differentially expressed when comparing *postnb*:CreER^{T2} lineage-traced cells at 7 dpi with those cells at 60 dpi (with the exception of the *kdrl*:mCherry population). Expression levels in the *wt1a*:GFP population are also shown for comparison. fpkm values were used. The list of genes encoding for secreted molecules was obtained by using Ingenuity software and manually adding the genes encoding for collagens and metalloproteinases not identified by Ingenuity. For better visualization of changes in gene expression between the two groups, values were scaled independently for each gene, that is, each row.

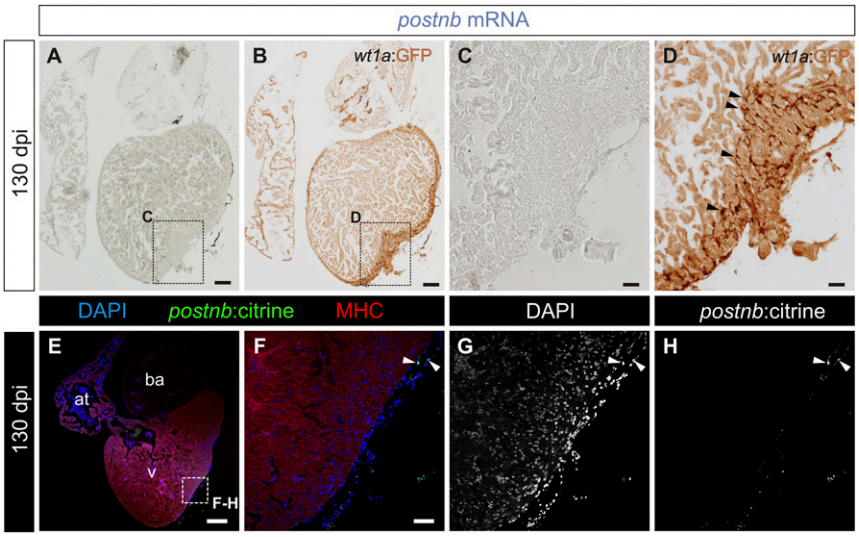

Fig. S8. Expression pattern of *wt1a*:GFP and *postnb*:citrine in fully regenerated hearts. (*A–D*) *postnb* mRNA in situ hybridization (purple) followed by anti-GFP immunohistochemistry (brown) of sections of *wt1a*:*GFP* ventricles at 130 dpi ($n = 3/3$). Arrowheads mark *wt1a*:GFP$^+$ cells. Sections were stained simultaneously with those shown in Fig. 1 *C–F*. (*E–H*) Immunofluorescence with anti-GFP (green) and anti-MHC (red) of a *postnb:citrine* heart section at 130 dpi ($n = 4/4$). Nuclei are counterstained with DAPI. Arrowheads mark GFP$^+$ cells. [Scale bars, 100 μm (*A*, *B*, and *E*) and 25 μm (*C*, *D*, and *F*).]

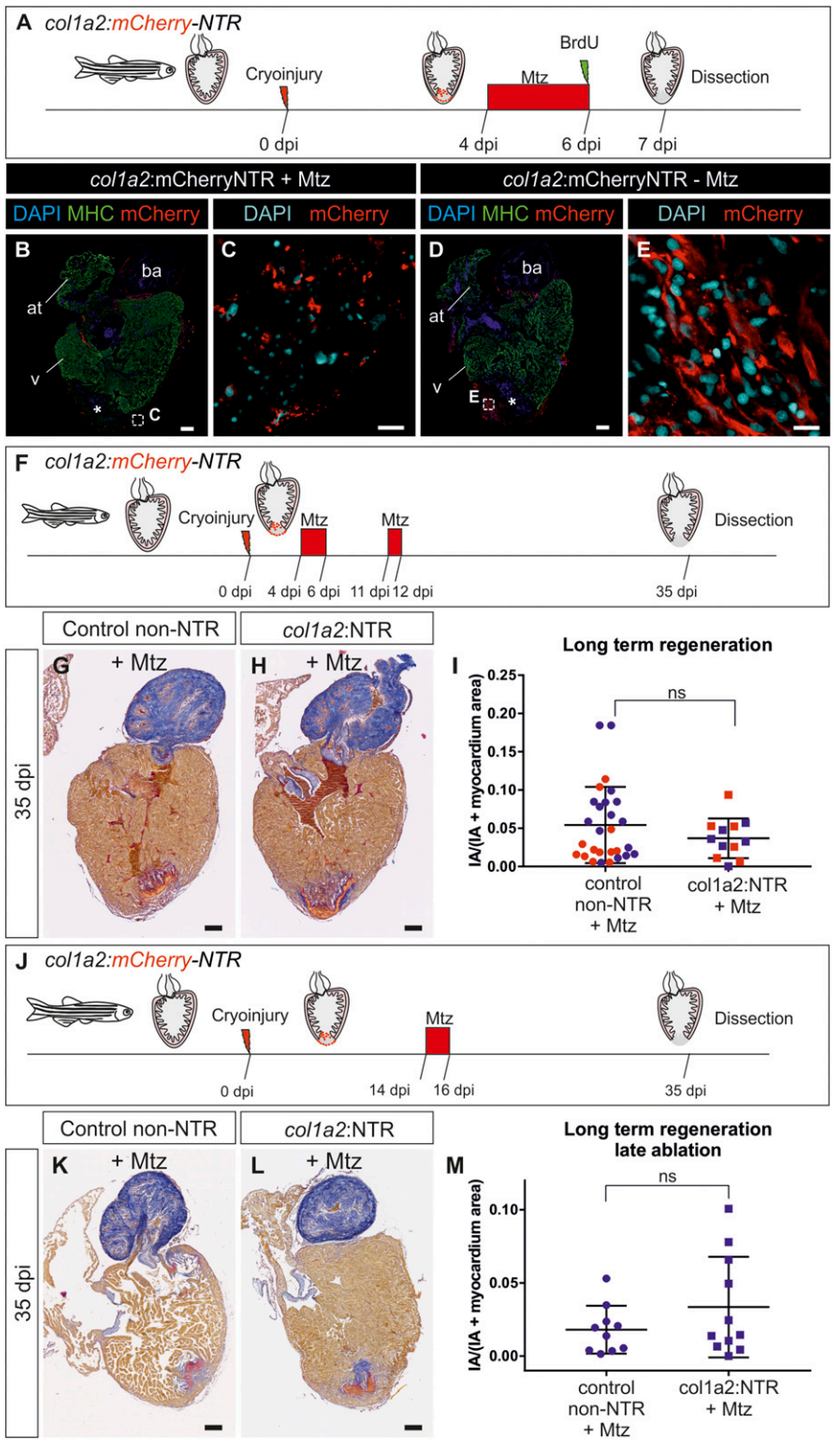

Fig. S9. Heart regeneration upon genetic ablation of *col1a2*-expressing cells. (*A*) *col1a2*:mCherry-*NTR* (in short *col1a2:NTR*) adult animals were cryoinjured and treated with Mtz from 4 to 6 dpi. BrdU injection was performed 1 d before fixation to assess cardiomyocyte proliferation. (*B*–*E*) Immunofluorescence of heart sections of *col1a2:mCherry-NTR* treated with Mtz (*B* and *C*) or untreated controls (*D* and *E*). mCherry, red; MHC, green; nuclei (DAPI), blue for *B* and *D*, and cyan for *C* and *E*. Asterisk, injured area. In Mtz-treated fish, *col1a2*:mCherry-NTR labels cells with fragmented nuclei and the homogeneous mCherry expression observed in the wild-type heart is lost. (*F*) Experimental scheme to study regeneration upon genetic ablation of *col1a2*-expressing cells. *col1a2:NTR* transgenic zebrafish were cryoinjured and treated with 10 mM Mtz between 4 to 6 and 11 to 12 dpi. Hearts were dissected at 35 dpi, sectioned, and stained with AFOG to determine the degree of regeneration. (*G* and *H*) AFOG-stained sagittal sections through ventricles of a Mtz-treated *col1a2:loxP-tagBFP-loxP-mCherry-NTR* heart (control) and a Mtz-treated *col1a2:NTR* heart. (*I*) Quantification of the injury area versus total ventricular area from 28 control hearts and 12 *col1a2:NTR* hearts. Blue and red colors indicate results from two independent experiments. Shown are individual measurements as well as mean and SD. No significant difference was observed between control and *col1a2:NTR* groups by unpaired Student's *t* test ($P = 0.75$). (*J*) Experimental scheme. *col1a2:NTR* transgenic zebrafish were cryoinjured and treated with 10 mM Mtz between 14 and 16 dpi. Hearts were dissected at 35 dpi, sectioned, and stained with AFOG to determine the degree of regeneration. (*K* and *L*) AFOG-stained sagittal sections through ventricles of a Mtz-treated *col1a2:loxP-tagBFP-loxP-mCherry-NTR* heart (control) and a Mtz-treated *col1a2:NTR* heart. (*M*) Quantification of the injury area versus total ventricular area from 10 control hearts and 11 *col1a2:NTR* hearts. Shown are individual measurements as well as mean and SD. No significant difference was observed between control and *col1a2:NTR* groups by unpaired Student's *t* test ($P = 0.2113$). (Scale bars, 100 μm.)

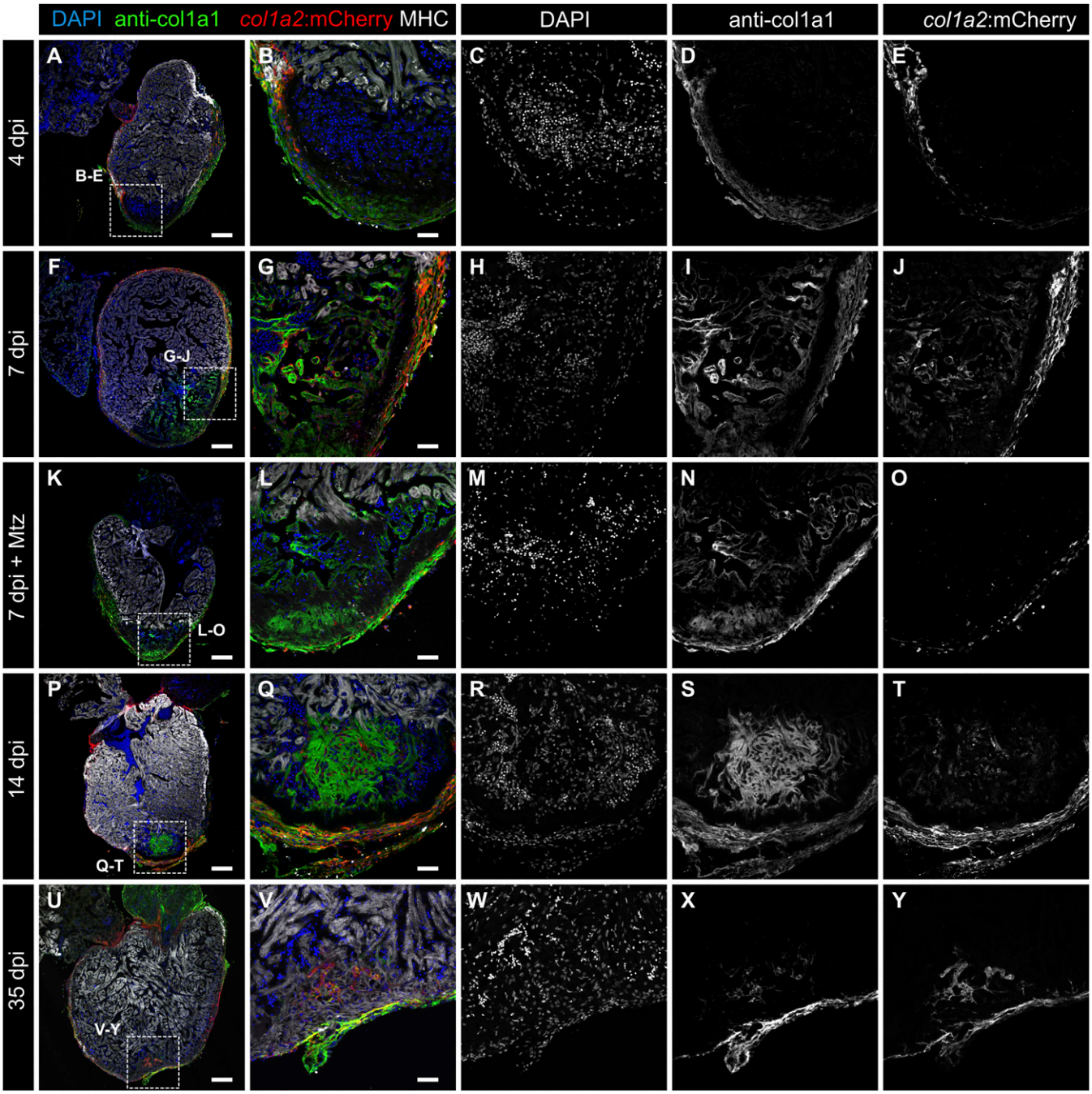

Fig. S10. Colocalization of *col1a2*:mCherry and anti-col1a1 at different stages postinjury and ablation. Sagittal sections through *col1a2:mCherry* hearts at 4 dpi (*A–E*; $n = 4/4$), 7 dpi (*F–J*; $n = 4/4$), 7 dpi treated with Mtz (*K–O*; $n = 4/4$), 14 dpi (*P–T*; $n = 4/4$), and 35 dpi (*U–Y*; $n = 3/3$). Sections were immunostained with anti-mCherry (red), anti-col1a1 (green), and anti-MHC (white). Nuclei were counterstained with DAPI (blue). [Scale bars, 25 μm (*B*, *G*, *L*, *Q*, and *V*) and 100 μm (*A*, *F*, *K*, *P*, and *U*).]

Table S1. Sequence information of primers

Primer no.	Primer name	Sequence
1	col1a2_HA1_loxP_F	aagtagttaaaccagggcactgcggcacaaggagtctgcatgtcggtttACCGGTGGATCCACTATAAC
2	col1a2_HA2_kanFRT_R	tacgaagtcactgcaagcagcaacagaatccgggtatccacaaagctgagGGAGGCTACCATGGAGAAG
3	postnb_HA1_citrine_F	cctcagctcaagcccatttcttgctctgaagtctcacagaggagaaagcaACCATGGTGAGCAAGGGCGAGGAG
4	postnb_HA2_kan_R	tcaaaggcagacagcacaaagagtgcaaaagtagctgcaaagaggagcttTCAGAAGAACTCGTCAAGAAGGCG
5	postnb_HA1_CreERT2_F	cctcagctcaagcccatttcttgctctgaagtctcacagaggagaaagcaaccatgTCCAACCTGCTGACTGTGCACC
6	postnb_HA2_kanFRT_R	tcaaaggcagacagcacaaagagtgcaaaagtagctgcaaagaggagcttGGAGGCTACCATGGAGAAG
7	pTarBAC_HA2_iTol2_AmpCryeCFP	cgcggggcatgactattggcgcgccggatcgatccttaattaagtctactaGAAACAGCTATGACCATGTAA
8	pTarBAC_HA1_iTol2_AmpCryeCFP	gcgtaagcggggcacatttcattacctctttctccgcacccgacatagatCCCTGCTCGAGCCGGGCCCAAGTG
9	pTarBAC_HA1_iTol2_F	gcgtaagcggggcacatttcattacctctttctccgcacccgacatagatCCCTGCTCGAGCCGGGCCCAAGTG
10	pTarBAC_HA2_iTol2_R	gcggggcatgactattggcgcgccggatcgatccttaattaagtctactaATTATGATCCTCTAGATCAGATC

Primers 1 to 10 were used for cloning of the DNA constructs used to generate the transgenic zebrafish lines. Red, homology arms. Green, minimal Kozak sequence. Capital letters, overlapping with template sequence. F, forward; R, reverse.

Table S2. Sequence information of genes

Gene	Forward primer	Reverse primer
col1a2	AGTGGAGCTTCTGGTCCAAG	CTCCCTTCACTCCAACAGGT
postnb	ATGAGACCCCAGGCTGAGT	TCCATGGACATCACCTCATC
EF1-alpha	CAGCTGATCGTTGGAGTCAA	TGTATGCGCTGACTTCCTTG
rps11	GATGGCGGACACTCAGAAC	CCAATCCAACGTTTCTGTGA

These primers were used for qPCR experiments.

Dataset S1. List of differentially expressed genes comparing *wt1a*:GFP$^+$ cells with the rest of the ventricular cells in uninjured zebrafish hearts

Dataset S1

Dataset S2. List of differentially expressed genes comparing *kdrl*:mCherry$^+$ cells from uninjured cardiac ventricles and cardiac ventricles at 7 dpi

Dataset S2

Dataset S3. List of differentially expressed genes comparing *postnb*:citrine$^+$ cells with the rest of the cells at 7 dpi

Dataset S3

Pools of apices of cardiac ventricles of the line *postnb:citrine;kdlr:mCherry* were homogenized to sort cells. Three groups of cells were isolated: *postnb*:citrine$^+$, *kdlr:mCherry*, and the rest of the cells. RNA was extracted and transcriptome analysis was performed to compare *postnb*:citrine$^+$ with the pool of the rest of the cells.

Dataset S4. List of differentially expressed genes comparing *postnb*-derived cells at 7 and 60 dpi

Dataset S4

Hydroxytamoxifen was added at 1 and 3 dpi to *postnb:CreERT2;ubb:Switch* adult zebrafish. GFP$^+$ *postnb*-derived cells were extracted from the apices of hearts at 7 and 60 dpi.

Dataset S5. Sequence information on the iTol2Amp-crystGFP plasmid

Dataset S5

Dataset S6. Sequence of the *fli1a:CreERT2* construct

Dataset S6

Dataset S7. Sequence information on the *wt1a:CreERT2* plasmid

Dataset S7